

Characterizing In and N impurities in GaAs from *ab initio* computer simulation of (110) cross-sectional STM images

Xiangmei Duan,^{1,*} Maria Peressi,^{1,2,†} and Stefano Baroni^{1,3}
¹CNR-INFM DEMOCRITOS National Simulation Center, Trieste, Italy
²Dipartimento di Fisica Teorica, University of Trieste, Trieste, Italy
³Scuola Internazionale Superiore di Studi Avanzati, Trieste, Italy
 (Received 6 September 2006; published 30 January 2007)

Computer simulations of cross-sectional scanning-tunneling microscopy images of GaAs(110) are performed by means of density-functional theory, with the aim of characterizing In_{Ga} and N_{As} substitutional impurities. In some cases the comparison between an experimental image taken at a single negative bias with the results of our simulations is sufficient to discriminate among different types and locations of impurities. When ambiguities arise, a combined positive/negative scan of the same region will help resolve them. We find that In_{Ga}-N_{As} neighboring pairs are energetically favored relative to the isolated impurities. The main features of the images of these pairs are determined by the location of the nitrogen atoms, but details due to neighboring indium atoms are also meaningful and recognizable in the experimental images.

DOI: 10.1103/PhysRevB.75.035338

PACS number(s): 73.20.-r, 73.43.Cd, 68.37.Ef

I. INTRODUCTION

In recent years GaAsN and InGaAsN alloys have captured a growing interest due to their remarkable properties and potential applications in optoelectronic devices and solar cells.^{1,2} The presence of only a few percent of nitrogen causes a strong band gap reduction with respect to the host material, determining a so-called *giant optical bowing* effect.^{3,4} Incorporation of both N and In in a GaAs host matrix potentially allows for a combined tuning of the band gap and lattice parameter by controlling the N/In ratio. In particular, an indium content of about 13% together with about 4.5% of nitrogen make InGaAsN conveniently lattice matched to GaAs.

Cross-sectional scanning tunneling microscopy (XSTM) (Ref. 5) has been recently applied to determine the distribution of N and/or In atoms in GaAsN and InGaAsN alloys,^{6,7} quantum wells,⁸ and quantum wires.⁹ There is a general agreement about the main characteristic features of N atoms substituting As (N_{As}) and In atoms substituting Ga (In_{Ga}): N_{As} is characterized by a dark spot at negative bias, similar to an As vacancy, very pronounced if it is on surface, less pronounced from the third subsurface layer; In_{Ga} gives rise to a bright spot at positive bias voltages. From XSTM images of In_xGa_{1-x}As_{1-y}N_y/GaAs quasi-lattice-matched quantum wells ($x=0.13$, $y=0.045$) acquired at positive and negative bias voltage, Duca *et al.*⁸ were able to identify fingerprints of on-surface In and N isolated impurities, as well as of In-N, N-N, and In-In pairs. In this way, however, only *on-surface* pairs can be clearly identified. The observed frequency of In-N pairs is larger than expected for a completely random distribution of the impurities, but less than predicted from Monte Carlo simulations.¹⁰ The In-N frequency could be even larger if also subsurface atoms could be identified and taken into account. Therefore, the characterization of In_{Ga}-N_{As} impurity pairs in In_xGa_{1-x}As_{1-y}N_y calls for a deeper investigation aimed at identifying specific features which will allow to unambiguously distinguish between isolated impurities and pairs thereof.

In this paper we perform such an investigation, based on a comparison between experimental XSTM images, and com-

puter simulations performed with state-of-the-art electronic-structure techniques, in the framework of the density functional theory and the plane-wave pseudopotential method. Our main conclusion is that, while images taken at negative bias may not contain sufficient information to distinguish an impurity pair from an isolated on-surface N_{As}, the combination of such an image with one taken at a reverse bias, thus sampling empty impurity states, would allow to discriminate between them.

II. COMPUTATIONAL DETAILS

We perform density-functional theory calculations in the local-density approximation (DFT-LDA), using the *ab initio* pseudopotential plane-wave method PWSCF code of the Quantum ESPRESSO distribution.¹¹ We use norm-conserving pseudopotentials from the Quantum ESPRESSO public table¹² with a plane-wave kinetic-energy cutoff of 20 Ry.¹³ The calculated structural and electronic properties of GaAs, both for bulk and (110) surface, and those of bulk zincblende GaN and InN, which are relevant because of the impurities, are of the same good quality as currently found in the literature.¹⁴ Most of the results reported here are obtained with supercells containing a GaAs slab of 6 atomic layers separated by a vacuum region equivalent to 5 atomic layers (~ 12 Å), with impurities on one surface and hydrogen on the other, saturating dangling bonds. Test calculations indicate that these sizes are enough to avoid the interaction between the two doped surfaces of the slab. The surface periodicity is 3×4 or 3×6 with 12 or 18 atoms, respectively, according whether impurities are studied individually or in pairs. A $3 \times 2 \times 2$ Monkhorst-Pack special k -point mesh for self-consistent calculations and a $6 \times 4 \times 4$ mesh for non-self-consistent calculations of densities of states and XSTM images are used. The surface geometry has been optimized by keeping only the hydrogen and the saturated GaAs layer fixed. Other technical details are similar to those of Ref. 21. With such details, the accuracy for the atomic positions is of the order of 0.01 Å, of same good quality as currently found in the literature.

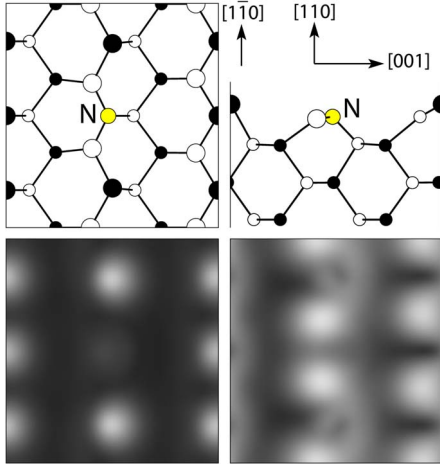


FIG. 1. (Color online) Isolated substitutional N_{As} impurity on (110) GaAs surface. Upper panel: top (left) and side (right) views of the atomic geometry with a ball and stick model. Big black and white spheres represent the surface As and Ga atoms, respectively, and smaller spheres indicate deeper atoms. Lower panel: STM images at $V_b = -1$ eV (left) and $V_b = 1$ eV (right).

XSTM images are simulated from the local density of states (LDOS) using the Tersoff-Hamann model,¹⁵ which approximates the tunneling current with:

$$I(V) \propto \int_{E_F}^{E_F + eV_b} LDOS(\mathbf{r}, \epsilon) d\epsilon, \quad (1)$$

where \mathbf{r} is the position of the tip, E_F is the Fermi energy, and V_b the applied bias. In this model neither the tip-surface interaction nor the particular shape of the tip are taken into account. More refined approaches are present in the literature,^{16–20} but despite its simplicity and the severe approximations used, the Tersoff-Hamann model has shown to be able to provide, at least qualitatively, a correct description of STM images in similar cases of defected III-V semiconductor surfaces. If not otherwise stated, we use $V_b = +1$ (–1) eV for positive (negative) bias.

III. RESULTS

A. Isolated N_{As} impurities

Nitrogen has a larger electronegativity and a smaller size than arsenic, therefore it produces lattice distortions and variations in the electronic density-of-states when it substitutes As. The side and top views of the relaxed atomic structure of an on-surface N_{As} impurity are shown in the top panel of Fig. 1. The most relevant features of the lattice structure are (i) a contraction of the Ga-N bond length (1.99 Å) with respect to that of Ga-As (2.38 Å); (ii) an inward displacement of the two surface Ga nearest neighbors (NN) of the N impurity towards N atom, with their relative distance decreased by 0.58 Å; (iii) an inward shift of the N impurity with respect to the surface As atoms, thus appearing like a depression. The corresponding fingerprint of N_{As} impurities in the XSTM images is a dark spot in the filled-state (negative-bias) image, like a depression, similar to surface

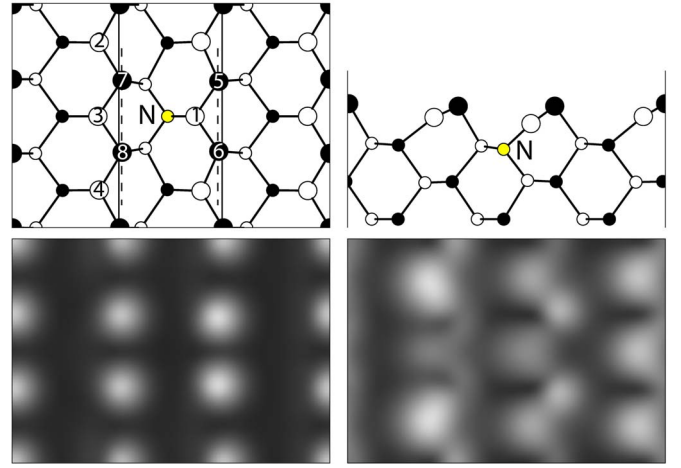


FIG. 2. (Color online) Isolated subsurface substitutional nitrogen impurity, N_{As} , in GaAs. See Fig. 1.

As vacancy, due to the combination of structural and electronic effects. This result confirms the interpretation of some experimental XSTM images reported in the literature.^{6–8} A characteristic feature also appears at positive-bias voltages, where the images of the empty states of the two surface Ga-NN's are closer to each other in the [110] direction. We notice that for this configuration, as well as for all the others that we have considered, the isovalent N_{As} and In_{Ga} impurities introduce only small modifications at the band edges and no midgap states, in agreement with what is reported in Ref. 6.

A local contraction of the lattice also occurs when N_{As} is in the second layer, as shown in Fig. 2. Surface As atoms which are next-nearest neighbors (NNN) to nitrogen are shifted toward the impurity: As(7) and As(8) on the left of the impurity are shifted by about 0.24 Å with respect to their regular position in the ideal surface, while As(5) and As(6) on the right of the impurity are shifted by about 0.18 Å.

The side view allows to appreciate the changes of the surface buckling due to the nearby Ga-As pairs. The buckling of Ga(1) with respect to its As NN is 0.87 Å (to be compared with 0.67 Å for the clean surface), while Ga(2) is buckled by 0.60 Å with respect to its As NN. The contraction of the distance of the surface As surrounding the impurity corresponds to a distortion in the row of the filled-states images that can be appreciated at negative bias ($V_b = -1.0$ eV), as also reported in Ref. 6. At positive bias ($V_b = +1.0$ eV), the surface Ga(1), which is NN to N, is slightly darker than Ga atoms further from the impurity. Such depression in the STM image can be explained easily by its inward displacement (0.27 Å). Ga(3) appears even darker than Ga(1), although not deeper than others with respect to the surface. In this case therefore the effect is purely electronic, as it can be inferred by examining the atomic-projected density of states: the empty states of Ga(3) are pushed towards higher energies, so that their contribution to positive-bias STM image [see Eq. (1)] is smaller than normal surface Ga atoms. The occupied states of Ga(2) and Ga(4) instead are shifted towards lower energies, thus increasing the contribution to the previous integral at positive bias and resulting in a brighter

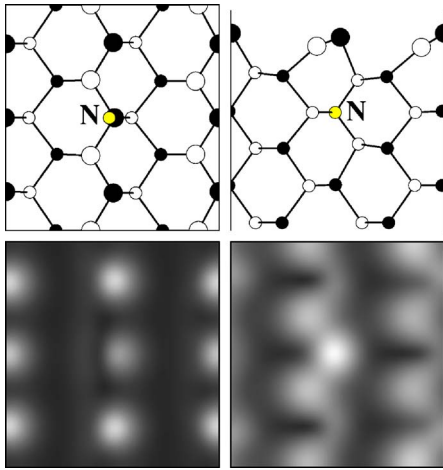


FIG. 3. (Color online) Isolated N_{As} impurity on the third layer from (110) GaAs surface. See Fig. 1.

image. Similar features are found in experimental images and interpreted along these lines.^{6,8}

The effect of a N impurity in the third layer is shown in Fig. 3. Lattice distortions are less pronounced, but still propagate from the impurity up to the surface. The surface As atom located above the N protrudes less with respect to other surface As atoms, with a buckling reduced to 0.46 Å. In correspondence to N_{As} the simulated XSTM image at negative bias voltage shows a depression (dark spot) similar, but less pronounced, to the case of surface N_{As} . The fingerprint of third-layer N_{As} is visible also at positive bias with an additional bright spot with respect to the rows of Ga empty states. Such spot originates from surface As located above the N, whose empty states are strongly modified and pushed towards lower energies, as it can be seen from the atomic-projected density of states. We notice that this additional bright spot at positive bias is at variance with what occurs for N_{As} on surface, thus allowing to distinguish between the two cases. The contrast of the features just described is attenuated by increasing the applied bias, both in the positive and in the negative directions, as it occurs for anion vacancies on (110) cleaved III-V surfaces.²²

B. Isolated In_{Ga} impurities

Let us come now to cationic impurities, In_{Ga} , i.e., In atoms at Ga sites. The In-As bond is longer than Ga-As and therefore lattice distortions also occur in this case. When In_{Ga} is on surface, the surface zig-zag bond chain accommodates to these distortions: the surface In-As bond length is 2.49 Å and In_{Ga} is slightly pushed outward (by about 0.07 Å farther than Ga atoms). Side and top views of the relaxed structure of on-surface In_{Ga} are shown in the top panel of Fig. 4: the impurity is visible with a brighter spot than Ga in the empty-state image (with a bias of +1.5 V or even higher). Our simulations confirm the interpretation of some experimental images reported in the literature.^{8,9,23}

Subsurface In_{Ga} also gives rise to lattice distortions: the bond between In_{Ga} and its NN surface As atom is 2.55 Å, longer than Ga-As (2.42 Å), so that the surface As atom is

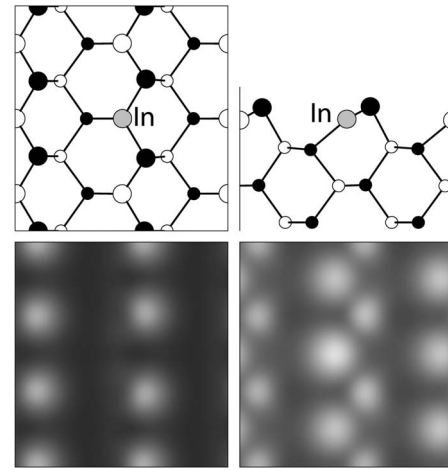


FIG. 4. Isolated In_{Ga} impurity on (110) GaAs surface. See Fig. 1. Lower panel: STM images at $V_b = -1$ eV (left) and $V_b = 2$ eV (right).

pushed outward from the surface by 0.18 Å. The result is a surface-As spot bright also at positive voltage in XSTM images, as shown in Fig. 5. A similar feature has also been observed in some experimental images.^{9,23}

Comparing the formation energies of on-surface and subsurface In_{Ga} configurations, we find no appreciable difference (only 0.06 eV) which is consistent with the experimental observation of no preferential distribution between the two layers.⁹

C. In_{Ga} - N_{As} pairs

The incorporation of both N and In into GaAs allows for the simultaneous tuning of the band gap and average lattice constant in the diluted $In_xGa_{1-x}As_{1-y}N_y$ quaternary alloy. Kim and Zunger¹⁰ have suggested that the preferential formation of In-N and Ga-As, relative to In-As and Ga-N bonds, results in a sizeable amount of short-range order. The existence of short-range order of this kind is confirmed by recent experimental evidence,^{8,24} although to a lesser extent

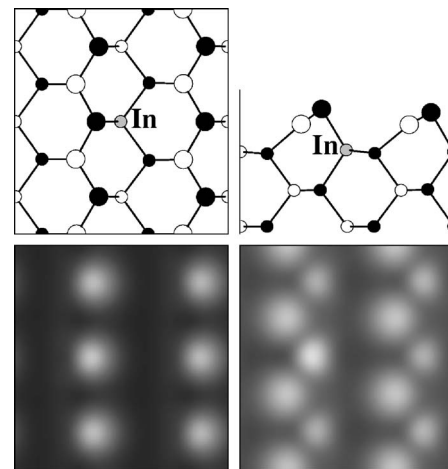


FIG. 5. Isolated subsurface substitutional impurity In_{Ga} in GaAs. See Fig. 4.

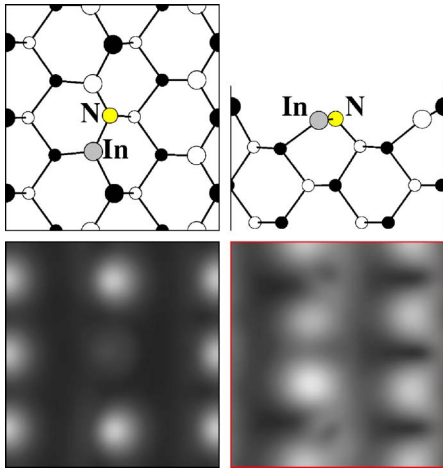


FIG. 6. (Color online) A defect pair with substitutional In_{Ga} and N_{As} both on surface layer (case A in the text). See Fig. 1.

than computer simulations would suggest.¹⁰ An accurate and unambiguous identification of In-N pairs in XSTM images is therefore crucial for a proper comparison between theory and experiment. In the following we present a systematic series of simulations of the images of In-N pairs for different locations in the first two (110) layers (on- and subsurface). There are four different possible such configurations: (A) both In_{Ga} and N_{As} are on-surface along the exposed zigzag bond chain; (B) both In_{Ga} and N_{As} are subsurface; (C) In_{Ga} is on surface and N_{As} subsurface, their projection on the surface being (001)-oriented; (D) the configuration complementary to C with N_{As} on-surface and In_{Ga} subsurface.

Side and top views of the equilibrium structure for configuration A are shown in the upper panel of Fig. 6. Along the exposed zigzag bond chain, the most relevant bond lengths close to the impurities are 2.13 Å for In-N, 2.55 Å for In-As, and 1.97 Å for Ga-N. These bonds give rise to a local distortion of the lattice. The lower panels of Fig. 6 show the occupied- (negative bias) and empty-state (positive bias) XSTM images of this configuration. The negative-bias image is characterized by a missing anion spot (corresponding to surface N_{As}), whereas a brighter cation spot is present in the positive-bias image (corresponding to surface In_{Ga}). At negative bias, the image is similar to that of an isolated surface N_{As} impurity, but at positive bias the image differs from that of either isolated N_{As} and In_{Ga} : the brighter spot generated by the impurity pair is in this case asymmetric.

Figure 7 shows case B, with both N_{As} and In_{Ga} subsurface. Some lattice distortion is also present here, although to a lesser extent than in the previous case. Surface Ga atoms bound to subsurface N_{As} go inward by 0.31 Å with respect to “regular” Ga atoms bound to As, also driving a small displacement of neighboring surface As atoms (about 0.12 Å with respect to the position of the “regular” As atoms). The most relevant bond lengths for In-N, Ga-N (on-surface), and In-As (on-surface) are 2.19 Å, 2.01 Å, and 2.56 Å, respectively. These lattice distortions give rise to a deformation of the rows of the anionic occupied-state images shown in the left-lower panel of Fig. 7 where we can see the anion bright spots slightly misplaced from their symmetrical position. In

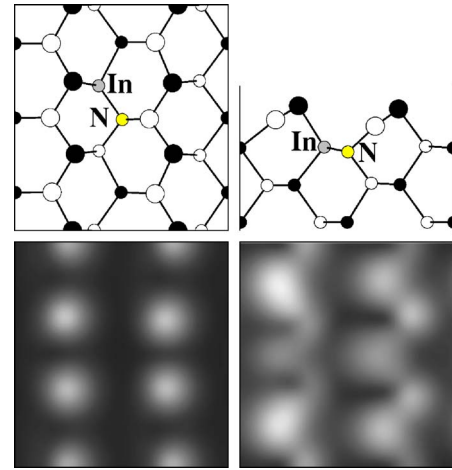


FIG. 7. (Color online) A defect pair with substitutional N_{As} and In_{Ga} both subsurface (case B in the text). See Fig. 1.

the empty-state images, at low bias voltage, we can recognize two brighter spots corresponding to two surface Ga atoms in the neighborhood of the impurities. Increasing the voltage, either at positive or negative bias, the contrast decreases and the above characteristic features are less visible.

Similar lattice distortions and similar features in the XSTM images occur for an on-surface In_{Ga} impurity with a subsurface N_{As} nearest neighbor (case C), as shown in Fig. 8. Also in this case the $\text{In}_{\text{Ga}}\text{-N}_{\text{As}}$ bond is shorter (2.15 Å) than Ga-As (2.37 Å), resulting in an inward displacement of the on-surface In_{Ga} larger by 0.25 Å than for Ga atoms. The empty-state XSTM image shows a less bright In_{Ga} spot than Ga atoms, whereas the two neighboring Ga spots in the adjacent row are enhanced.

A sizable contraction in the zigzag bond chain exposed at the surface occurs when an on-surface N_{As} impurity has an In_{Ga} subsurface nearest neighbor (case D), as shown in Fig. 9. In this case the N_{As} impurity relaxes outward less (by 0.4 Å) than on-surface As atoms, and it shifts by 0.23 Å along the [001] direction, with the $\text{In}_{\text{Ga}}\text{-N}_{\text{As}}$ (2.14 Å) and Ga- N_{As} bonds (1.98 Å) shorter than Ga-As. The low-

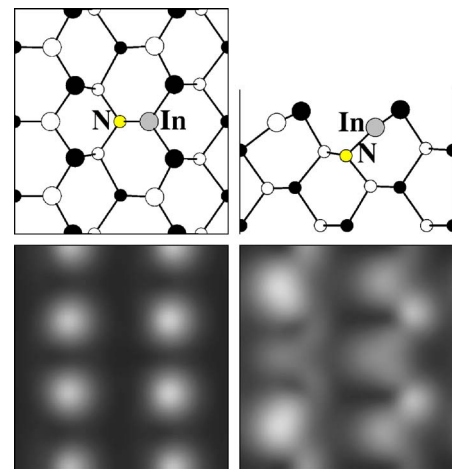


FIG. 8. (Color online) A defect pair with substitutional In_{Ga} on surface and N_{As} subsurface (case C in the text). See Fig. 1.

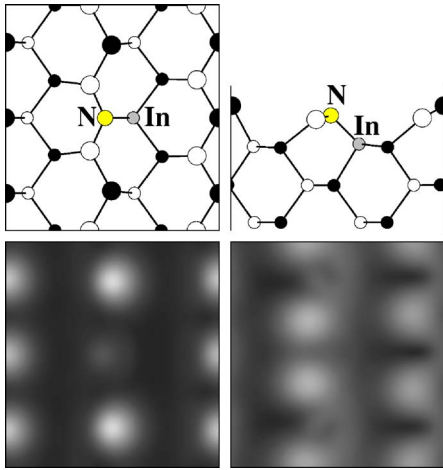


FIG. 9. (Color online) A defect pair with substitutional N_{As} on surface and In_{Ga} subsurface (case D in the text). See Fig. 1.

voltage negative-bias image depicts the N_{As} impurity as darker (depressed) and shifted along $[001]$, in between two brighter spots produced by the two NNN As atoms. In the positive-bias image, two brighter and closer spots are originated by Ga atoms nearest neighbors to N_{As} .

We now briefly report on the energetics of the various impurity configurations considered in the present work. We caution the reader that, since the experimentally studied surfaces are obtained by cleavage, the actual configurations of the impurities are not uniquely determined by their relative energy differences in presence of the surface; The energetics of the different possible configurations before cleavage, i.e., in bulk, plays also a fundamental role, as well as other factors during and after cleavage may affect the exposed surfaces. Nevertheless, it is interesting to discuss the energetics in presence of the surface and to investigate whether there are some very unfavorable and unstable configurations obtained after cleavage that could likely change.

In Table I, we report our calculated impurity formation energies. We see that the on-surface and subsurface configurations of isolated In_{Ga} are almost degenerate, so that we do

TABLE I. Relative formation energies of various impurity configurations considered in the present work. All the energies are referred to those of the most stable configurations (isolated subsurface impurities or pairs thereof).

Defect configuration	ΔE (eV)
In_{Ga} surf	0.06
In_{Ga} subsurf	-
N_{As} surf	0.15
N_{As} subsurf	-
N_{As} 3rd layer	0.28
A	0.28
B	-
C	0.14
D	0.36

not expect any substantial rearrangement after cleavage and annealing. For isolated N_{As} the subsurface location is the most favorable, followed by the on-surface and the third-layer subsurface configurations with energy differences within 0.3 eV/impurity. Such small energy differences are consistent with the lack of any experimental evidence of outward diffusion from the bulk toward the exposed surface or subsurface layer.^{6,8}

Concerning the $In_{Ga}-N_{As}$ pairs, our calculations predict configuration B ($In_{Ga}-N_{As}$ subsurface) to be the most stable, followed by C, A, and D at an energy 0.14, 0.28, and 0.36 eV higher, respectively. We notice that the greatest stability of configuration B is consistent with the greatest stability of the isolated subsurface In_{Ga} and N_{As} impurity configurations. The binding energies resulting from the difference between the pair configurations and the infinitely separated impurities indicate an attraction between the In and N impurities. This behavior is consistent with experimental findings⁸ and previous theoretical results obtained for the bulk alloy.^{10,25} Our calculated binding energy is 0.35 eV in case B and 0.44 eV in the bulk, the latter in perfect agreement with the value reported in Ref. 25. Considering also case A, with binding energy of 0.07 eV obtained by difference from case B, our findings indicate that the pair binding energy progressively decreases from the bulk towards the surface. Since the dominant, attractive contribution to $In_{Ga}-N_{As}$ bond is due to strain,^{24,25} whereas the chemical one is repulsive,²⁵ this trend can be explained considering that on surface the strain can be better accommodated and its attractive contribution reduced. Our results could also partially explain that the average number of In-N bonds observed in the cross-sectional surface of real samples⁸ is higher than expected for a random distribution but lower than theoretically predicted for the bulk.¹⁰

IV. CONCLUSIONS

We have presented a systematic study of the GaAs(110) cross sectional surface containing N and In dopants, performed using first-principles density-functional theory calculations. Our main result is the suggestion that a combination of negative/positive bias imaging of a doped region can help distinguish between different configurations that would otherwise appear similar if taken only at a negative voltage. This result highlights the power of *computational microscopy* as a powerful tool for the characterization of materials which provides information complementary to that obtained in the laboratory and essential for a proper interpretation of the latter.

ACKNOWLEDGMENTS

We would like to thank Silvio Modesti for prompting our interest in this problem and for many fruitful discussions. This work was supported by the Italian National Institute for the Physics of Matter (INFN) within the PRA-XSTMS project. Part of the computational resources were provided by the “Iniziativa Trasversale di Calcolo Parallelo” of the Italian Consiglio Nazionale delle Ricerche–Istituto Nazionale per la Fisica della Materia (CNR-INFN) and by the University of Trieste through an agreement with the CINECA supercomputing center in Bologna.

*Present address: School of Physics, The University of Sydney, Sydney 2006, Australia.

†Electronic address: peressi@ts.infn.it

- ¹F. A. Ponce and D. P. Bour, *Nature (London)* **386**, 351 (1997).
²M. Kondow, K. Uomi, A. Niwa, T. Kiatani, S. Watahiki, and Y. Yazawa, *Jpn. J. Appl. Phys., Part 1* **35**, 1273 (1996).
³J. Neugebauer and C. G. Van de Walle, *Phys. Rev. B* **51**, 10568 (1995).
⁴S.-H. Wei and A. Zunger, *Phys. Rev. Lett.* **76**, 664 (1996).
⁵By cross-sectional STM we mean scanning-tunneling microscopy of a surface cleaved *perpendicularly* to the growth axis of a sample grown epitaxially.
⁶H. A. McKay, R. M. Feenstra, T. Schmidling, U. W. Pohl, and J. F. Geisz, *J. Vac. Sci. Technol. B* **19**, 1644 (2001).
⁷H. A. McKay, R. M. Feenstra, T. Schmidling, and U. W. Pohl, *Appl. Phys. Lett.* **78**, 82 (2001).
⁸R. Duca, G. Ceballos, C. Nacci, D. Furlanetto, P. Finetti, S. Modesti, A. Cristofoli, G. Bais, M. Piccin, S. Rubini, F. Martelli, and A. Franciosi, *Phys. Rev. B* **72**, 075311 (2005).
⁹M. Pfister, M. B. Johnson, S. F. Alvarado H. W. M. Salemink, U. Marti, D. Martin, F. Morier-Genoud, and F. K. Reinhart, *Appl. Phys. Lett.* **67**, 1459 (1995).
¹⁰K. Kim and A. Zunger, *Phys. Rev. Lett.* **86**, 2609 (2001).
¹¹<http://www.pwscf.org> and <http://www.quantum-espresso.org>
¹²Norm-conserving pseudopotentials from the publicly available Quantum ESPRESSO table are used: N.pz-vbc.UPF, As.pz-bhs.UPF, Ga.pz-bhs.UPF, In.pz-bhs.UPF.

- ¹³Tests with higher cutoff (30 Ry) have been performed. The simulated XSTM images, which are the main focus of this work, do not change. Relative formation energies and binding energies, discussed in the text, change at most by 0.05 eV.
¹⁴C. Stampfl and C. G. Van de Walle, *Phys. Rev. B* **59**, 5521 (1999).
¹⁵J. Tersoff and D. R. Hamann, *Phys. Rev. Lett.* **50**, 1998 (1983); *Phys. Rev. B* **31**, 805 (1985).
¹⁶C. J. Chen, *Phys. Rev. Lett.* **65**, 448 (1990); *Phys. Rev. B* **42**, 8841 (1990).
¹⁷M. Chen, P. G. Clark, Jr., T. Mueller, C. M. Friend, and E. Kaxiras, *Phys. Rev. B* **60**, 11783 (1999).
¹⁸M. Di Ventura and S. T. Pantelides, *Phys. Rev. B* **59**, R5320 (1999).
¹⁹K. Cho and J. D. Joannopoulos, *Phys. Rev. Lett.* **71**, 1387 (1993).
²⁰S. H. Ke, T. Uda, R. Pérez, I. Stich, and K. Terakura, *Phys. Rev. B* **60**, 11631 (1999).
²¹X. Duan, M. Peressi and S. Baroni, *Phys. Rev. B* **72**, 085341 (2005); X. Duan, S. Baroni, S. Modesti, and M. Peressi, *Appl. Phys. Lett.* **88**, 022114 (2006).
²²G. Schwarz, A. Kley, J. Neugebauer, and M. Scheffler, *Phys. Rev. B* **58**, 1392 (1998).
²³K. J. Chao, C. K. Shih, D. W. Gotthold, and B. G. Streetman, *Phys. Rev. Lett.* **79**, 4822 (1997).
²⁴M. Ramsteiner, G. Mussler, P. Kleinert, and K. H. Ploog, *Appl. Phys. Lett.* **87**, 111907 (2005).
²⁵O. Rubel, K. Volz, T. Torunski, S. D. Baranovskii, F. Grosse, and W. Stolz, *Appl. Phys. Lett.* **85**, 5908 (2004).